JNeurosci
THE JOURNAL OF NEUROSCIENCE

Research Articles | Systems/Circuits

Neural Responses to Unexpected Stimulus Repetitions and Omissions in Auditory Cortex Provide Mixed Evidence for Predictive Coding

https://doi.org/10.1523/JNEUROSCI.0545-26.2026

Received: 27 March 2026
Revised: 5 October 2026
Accepted: 10 October 2026

Copyright © 2026 the authors

This Early Release article has been peer reviewed and accepted, but has not been through the composition and copyediting processes.The final version may differ slightly in style or formatting and will contain links to any extended data.

Alerts: Sign up at www.jneurosci.org/alerts to receive customized email alerts when the fully formatted version of this article is published.

Neural Responses to Unexpected Stimulus Repetitions and Omissions in Auditory Cortex Provide Mixed Evidence for Predictive Coding

Bhanu Shukla[1], Harry Shirley[1], Liad Goodovitch[1], Yonatan I. Fishman[2], and Yale E. Cohen[3]

[1]Department of Otorhinolaryngology, University of Pennsylvania, Philadelphia, PA 19104 USA

[2]Departments of Neurology and Neuroscience, Albert Einstein College of Medicine, Bronx, NY 10461, USA

[3]Departments of Otorhinolaryngology and Bioengineering, University of Pennsylvania, Philadelphia, PA 19104 USA

Running title: Mixed Evidence for Predictive Coding in A1

Corresponding author:
Yale E. Cohen, PhD
Department of Otorhinolaryngology
3400 Spruce St, 5 Ravdin
Philadelphia, PA 19147
Email: ycohen@pennmedicine.upenn.edu

Abstract word count: 140
Significance statement word count: 77
Introduction word count: 654
Discussion word count: 1232
Number of figures: 8

Acknowledgments: The authors want to thank Dr. Corey Roach for his help with stimulus development and analysis.

Conflicts of interest: The authors declare no conflicts of interest

Funding sources: This work was supported by a grant from the NIDCD-NIH.

Author contributions: BS, YF, and YEC designed the research; BS and HS performed the research; BS, LG, YF, and YEC analyzed data; BS, LG, HS, YF, and YEC wrote the paper

J Neurosci Accepted Manuscript

Abstract

Humans and other animals process sensory uncertainty by integrating stimulus information with prior knowledge and expectations. Predictive coding conceptualizes perception as a form of Bayesian inference wherein hierarchical brain circuits update internal models to reconcile bottom-up sensory input with top-down predictions. Whereas predictive coding is a leading theory, the extent to which it is implemented in primary sensory cortices remains a matter of debate. To further investigate this issue, we examined single-neuron spiking activity in male macaque primary auditory cortex (A1) to expected versus unexpected stimulus repetitions and to expected versus unexpected stimulus omissions. On average, we found that A1 neurons did not show enhanced responses to unexpected stimulus repetitions, contrary to predictive-coding theory. However, they did show enhanced responses to unexpected stimulus omissions. Taken together, these mixed results place empirical constraints on how predictive coding is implemented in A1.

JNeurosci Accepted Manuscript

Significance Statement

Perception depends on the brain's ability to infer the causes of sensory inputs by integrating new information with prior knowledge under uncertainty. Our results reveal nuanced evidence for predictive coding within the primary auditory cortex (A1). Specifically, spiking activity during unexpected stimuli and unexpected stimulus omissions provide conflicting and supporting data, respectively, for this Bayesian framework. These findings refine our understanding of neural mechanisms underlying perception and provide empirical constraints on the neurobiological implementation of predictive processing.

JNeurosci Accepted Manuscript

Introduction

Humans and other animals generate perceptual representations of the world to guide adaptive behavior despite uncertainty in sensory input (Knill and Richards, 1996; Gold and Shadlen, 2002; Gold and Shadlen, 2007; Griffiths and Tenenbaum, 2011; Aitchison and Lengyel, 2017; Heilbron and Chait, 2018). Perception can be considered a process by which this sensory uncertainty is integrated with prior knowledge in a manner that follows the rules of Bayesian inference. In hearing, for example, such inference is crucial for learning language, parsing speech in noisy environments, and music appreciation (Denham and Winkler, 2006; Szabó et al., 2016; Zarcone et al., 2016; Koelsch et al., 2019).

One highly influential neural implementation of Bayesian inference is “predictive coding” (PC) (Rao and Ballard, 1999; Friston, 2005; Shipp, 2016; de Lange et al., 2018; Heilbron and Chait, 2018). Under the PC framework, internal perceptual models are updated based on “surprise” (i.e., “prediction-error”) responses, which are elicited when there is a mismatch between “bottom-up” sensory input and “top-down” expectations (i.e., predictions). However, there is an active debate as to whether and to what extent PC is implemented in the auditory cortex (Parras et al., 2017; Carbajal and Malmierca, 2018; Heilbron and Chait, 2018; Teichert et al., 2025). A key question in this debate is whether putative prediction-error responses can explained more parsimoniously by local bottom-up neurophysiological phenomena such as stimulus-specific adaptation (SSA), forward suppression, or “off” responses (May and Tiitinen, 2010; Fishman, 2014; Aitchison and Lengyel, 2017; Symonds et al., 2017; Heilbron and Chait, 2018; Ross and Hamm, 2020; May, 2021; O'Reilly, 2021).

Here, we expanded upon previous efforts to differentiate PC from local bottom-up mechanisms (e.g., SSA) by recording from the primary auditory cortex (A1) of macaque

JNeurosci Accepted Manuscript

monkeys during auditory “pattern” and “omission” stimulus paradigms (Alain et al., 1994; Hughes et al., 2001; Wacongne et al., 2011; Wacongne et al., 2012; Fishman, 2014). During the pattern paradigm, we presented two different tone-burst sequences (see Fig. 2). The first sequence was a temporal sequence of identical tone-burst pairs separated by silence, which generated an expectation for tone-burst repetition (Alain et al., 1994; Macdonald and Campbell, 2011; Wacongne et al., 2011; Wacongne et al., 2012; Paavilainen, 2013). In contrast, the second was a temporal sequence of tone-burst pairs that alternated in frequency, which generated an expectation for tone-burst alternation. This expectation was then violated by the rare and unexpected repetition of one of the tone bursts. PC predicts enhanced responses to the unexpected repetition of the auditory stimulus. In contrast, SSA predicts reduced responses. During the omission paradigm, we also used two tone-burst sequences (Hughes et al., 2001) (Fig. 2). The first sequence consisted of the same-frequency tone-burst pairs, but the second tone burst in the pair was omitted 100% of the time; this generated an expectation for omission. In contrast, the second sequence contained identical tone-burst pairs separated by silence, which generated an expectation for tone-burst repetition. This expectation for repetition was then violated by the rare and unexpected omission of the second tone burst in the pair. Like with the pattern stimulus paradigm, PC predicts enhanced responses to the unexpected stimulus omission. This enhanced response cannot readily be explained by SSA because SSA results from the repetition of physically presented stimuli and not the absence of a stimulus.

Contrary to PC theory, our results did not reveal reliable evidence for enhanced responses to unexpected stimulus repetitions in A1. On the other hand and consistent with PC, we found that unexpected stimulus omissions elicited stronger responses than expected ones; these stronger responses could reflect either a prediction-error signal or a neural

JNeurosci Accepted Manuscript

121 correlate of a top-down prior expectation (Bendixen et al., 2009; Wacongne et al., 2011;
122 Sanmiguel et al., 2013a; Kok et al., 2014; Schröger et al., 2015; Chennu et al., 2016; de
123 Lange et al., 2018; Heilbron and Chait, 2018; Demarchi et al., 2019; Yaron et al., 2025).
124 These mixed results place empirical restraints on how PC is implemented in A1.
125
126

JNeurosci Accepted Manuscript

Materials and Methods

The University of Pennsylvania Institutional Animal Care and Use Committee approved all the experimental protocols in accordance with National Institutes of Health guidelines. The authors were not blind to group allocation during the experiment and when we analyzed the data outcomes.

All surgical procedures were conducted under general anesthesia and using aseptic surgical techniques. Two adult male rhesus macaques (*Macaca mulatta*; monkey W [14 years old] or monkey C [14 years old]) participated in this study. The monkeys were group housed and were maintained under water-controlled conditions during training and recording periods.

Before surgery, we identified the stereotactic location of the core auditory cortex (A1) through anatomical MRI scans (Romanski and Goldman-Rakic, 2002; Cohen et al., 2004; Frey et al., 2004; Johnston et al., 2016; Christison-Lagay et al., 2017). Using these scans, we designed a titanium recording chamber (Rogue, Inc) that was oriented perpendicular to the cortical layers of A1 (Frey et al., 2004; Banno et al., 2023; Cai et al., 2025). During surgery, we placed the monkey in a frameless stereotaxic device, removed the cranium over A1, and placed and secured the titanium chamber on the skull with titanium bone screws. Further details regarding the surgical approach can be found in Johnston et al. (Johnston et al., 2016).

We functionally defined A1 through two different complementary approaches (Banno et al., 2023; Cai et al., 2025). First, because we oriented our electrode array orthogonal to A1's cortical lamina, we identified A1 recording sites by their characteristic laminar response profile, including current-source density (CSD; the second spatial derivative, relative to electrode-contact separation, of the local-field potential) and the spatial pattern of multiunit

JNeurosci Accepted Manuscript

activity across the electrode contacts in a given penetration (Fig. 1) (Freeman and Nicholson, 1975; Nicholson and Freeman, 1975; Fishman et al., 2001a; O'Connell et al., 2014; Banno et al., 2023). Second, the anatomical arrangement of best frequencies obtained in different recording sessions was consistent with the anteroposterior tonotopic gradient characteristic of A1.

Experimental chamber

In each session, a monkey was seated in a primate chair. We placed a calibrated free-field speaker (MICRO [Gallo Acoustics]) 1 m in front of the monkey and at the monkey's eye level. Calibrated auditory stimuli were generated with Matlab (Mathworks), passed through a digital-to-analog converter (E22, Lynx Studio Technology Inc), and presented through the free-field speaker. These sessions took place in an RF-shielded room with sound-attenuating walls and echo-absorbing foam on the inner walls.

Auditory stimuli and paradigms

We presented dynamic moving ripple noise to determine a neuron's spectrotemporal response field (STRF). From this response field, we calculated the site's best frequency (BF; see *Neural analyses* below). On a day-by-day basis, we incorporated the BF into the frequency values of the tone bursts comprising the oddball, pattern, and omission paradigms (Fig. 2). In the pattern and omission paradigms, we established statistical regularities and violated those expectations. These paradigms, and our analyses of neural responses, were designed specifically to control for lower-level neurophysiological phenomena such as stimulus-specific adaptation, which cannot be distinguished from genuine prediction-error

JNeurosci Accepted Manuscript

responses utilizing the classic oddball paradigm. The “pattern” paradigm tests for prediction-error responses elicited by unexpected tone-burst repetitions. In contrast, the “omission” paradigm tests for prediction error or prediction-related responses elicited by unexpected tone-bust omissions (Wacongne et al., 2011; Schröger et al., 2015; Chennu et al., 2016). During recording sessions in which we utilized the oddball and the pattern or omission paradigms, the tone bursts had a 200-ms duration. During those sessions in which only the pattern and omission paradigms were presented, the tone bursts had a 100-ms duration to match previous studies (Fishman, 2014). All tone bursts had 10-ms linear on/off ramps and were presented at 65-75 dB SPL. The time between the offset and onset of the tone bursts in the oddball paradigm was 100 ms as was the time between the offset and onset of a tone-burst pair in the pattern and omission paradigm. The time between the offset of a tone-burst pair and the onset of the subsequent tone-burst pair was 300 ms. Even when we omitted a tone burst (see below), we maintained the timing between subsequent tone bursts.

DYNAMIC MOVING RIPPLE (DMR) NOISE. DMR noise is a continuous time-varying broadband noise stimulus that covers the frequency range between 0.1 and 32 kHz (10-min duration; 65-dB spectrum level per ⅓ octave; 96-kHz sampling rate; 24-bit resolution) (Escabí and Schreiner, 2002; Escabi et al., 2014). At any instant of time, the stimulus has a sinusoidal spectrum; the density of the spectral peaks is determined by the spectral modulation frequency (Ω = 0-4 cycles/octave). The peak-to-peak amplitude of the ripple is 30 dB. The stimulus also contains temporal modulations (F_m = 0-25 Hz). Both the spectral and temporal parameters vary randomly and dynamically; the maximum rates of change are 0.25 Hz and 1 Hz, respectively.

ODDBALL PARADIGM. This paradigm consisted of the repeated presentation of a tone burst at the same frequency value with the random presentation of a second “oddball” tone

JNeurosci Accepted Manuscript

198 burst at a different frequency value. In the standard pattern, the frequency of the standard
199 was set to the BF, and the frequency of the oddball was set a value that elicited half of the
200 firing rate elicited by the BF tone burst. In the “violation” version, the roles of the frequencies
201 were reversed, with the standard frequency set at a value that elicited half of the firing rate
202 elicited by the BF tone burst, whereas the oddball was set to the BF.

203 PATTERN PARADIGM. This paradigm used two different tone-burst sequences. The
204 first consisted of a temporal sequence of identical tone-burst pairs separated by silence,
205 which generated an expectation for tone-burst repetition (the “standard” pattern paradigm];
206 Fig. 2) (Alain et al., 1994; Macdonald and Campbell, 2011; Wacongne et al., 2011;
207 Wacongne et al., 2012; Paavilainen, 2013; Fishman, 2014). The second was a temporal
208 sequence of tone-burst pairs that alternated in frequency, which generated an expectation
209 for tone-burst alternation. This expectation was then violated by the rare and unexpected
210 repetition of one of the tone bursts (the “violation” pattern paradigm). The frequency of the
211 first tone burst in the pair was set to the BF of the recording site. The frequency of the second
212 tone-burst was set to a frequency value that elicited a neural response that was
213 approximately half of that elicited by the BF tone burst (Fishman and Steinschneider, 2012).

214 OMISSION PARADIGM. This paradigm used two tone-burst sequences conceptually
215 similar to those used in earlier studies of omission responses in humans (Hughes et al.,
216 2001). The first sequence consisted of the same-frequency tone-burst pairs, but the second
217 tone burst in the pair was omitted 100% of the time; this generated an expectation for
218 omission (the “standard” omission paradigm; Fig. 2). In contrast, the second sequence
219 consisted of identical tone-burst pairs separated by silence, which generated an expectation
220 for tone-burst repetition. This expectation for repetition was then violated by the rare,

JNeurosci Accepted Manuscript

unexpected omission of the second tone burst in the pair (the “violation” omission paradigm; Fig. 2). The frequencies of the tone bursts were set to the site’s BF.

Recording methodology and strategy

During a recording session, we first penetrated the dura with a stainless-steel guide tube (508-µm inner diameter) and advanced a 24-contact v-probe with 100-µm inter-contact spacing (Plexon) through the guide tube and into the brain. Neural signals were sampled at 24 kHz, filtered (0.003-6 kHz; PZ5-128, -64, RZ2, and RS4, TDT Inc.), and stored for online and offline analysis.

While advancing the electrode, we presented an auditory “search stimulus” (an 80-ms white-noise burst at 65 dB SPL). When auditory-evoked responses were detected, we calculated the CSD profile from the neural activity generated from ~110 repetitions of the search stimulus. Based on the CSD and multiunit activity (MUA) profiles, we adjusted the v-probe depth so that the electrode contacts with the highest MUA rates (Fig. 1A-C) and largest initial short-latency current sink were positioned in the middle contacts of the probe. This sink corresponds to extracellular current flow associated with postsynaptic potentials in stellate and pyramidal neurons within the thalamorecipient zone (lamina four and lower lamina) (Freeman and Nicholson, 1975; Nicholson and Freeman, 1975). Auditory responses were initially observed only on the channels nearest to the electrode tip, whereas more superficial contacts showed no response. Consequently, our baseline CSD profiles deviated from existing literature (Freeman and Nicholson, 1975; Nicholson and Freeman, 1975). However, as we advanced deeper, the profile changed and ultimately became consistent with the published literature. Once this target depth was identified, we retracted the electrode by 250–500 µm and allowed the tissue to stabilize for ≥60 minutes to reduce electrode drift.

JNeurosci Accepted Manuscript

Next, we recorded neural activity while the monkey passively listened to the DMR stimulus (Escabí and Schreiner, 2002; Miller et al., 2002). We used this neural activity to generate the STRFs from isolated single-unit spiking activity and calculate the neuron's BF. Next, we collected neural activity while monkeys listened to tone bursts presented within the context of the oddball, pattern, and/or omission paradigms. We presented the deviant stimuli either at consistent intervals within the violation variants of the paradigms (see Fig. 2) or at random times; in either case, deviant stimuli were only presented on 10–20% of the trials (i.e., with a probability of 0.1 to 0.2 during random presentation). Typically, during oddball trials, we presented ~900 standard sequences and 100 deviant sequences to the monkey. During pattern and omission trials, we presented 1000 standard sequences and 50-100 deviant sequences.

Finally, at the end of each session, we recomputed both the site's laminar CSD profile and the single-unit STRFs. We only report data from sessions in which the CSD and the STRFs were stable over the duration of the recording session; we found that >90%+ of the sessions were stable. We delivered rewards manually and randomly throughout the recording session to help to ensure that the monkey remained awake.

Neural analyses

EXTRACTION OF NEURAL SIGNALS. Local-field potentials (LFPs) were extracted by first low-pass filtering the neural signal (300-Hz cut-off frequency; four-pole bidirectional Butterworth filter) and then resampling the filtered signals at 1 kHz (Ghazanfar et al., 2005; Ghazanfar et al., 2008; Chandrasekaran and Ghazanfar, 2009; Tsunada et al., 2011; Gifford et al., 2019; Chiang et al., 2020). Multiunit activity (MUA) was extracted by filtering the neural signal (0.5-3.0 kHz), full-wave rectifying it, and then low-pass filtering (<0.6 kHz) to extract

JNeurosci Accepted Manuscript

the envelope of summed action-potential activity (Lakatos et al., 2005; Kayser et al., 2007; Steinschneider et al., 2008; Fishman and Steinschneider, 2009). After high-pass filtering (0.6- 6.0 kHz) the neural signal, single-unit spiking activity was sorted using Kilosort3 (Pachitariu et al., 2023). We used standard metrics to ensure high-quality single-neuron isolation (Schmitzer-Torbert et al., 2005; Liu et al., 2014).

GENERATION OF A NEURON'S SPECTROTEMPORAL RESPONSE FIELD (STRF) AND DETERMINATION OF BEST FREQUENCY (BF). We derived each neuron's STRF using the reverse-correlation method, which is the average spectrotemporal stimulus envelope immediately preceding each spike elicited by the DMR stimulus (Miller et al., 2001; Escabí and Schreiner, 2002). A STRF's "best frequency" (BF) was the frequency value that consistently elicited the largest neural response (Hermes et al., 1981; Kim and Young, 1994; Miller et al., 2001; Miller et al., 2002).

We utilized a two-step procedure to identify each STRF's reliable samples and its overall reliability (Escabi et al., 2014). To identify each STRF's significant spectrotemporal samples, we generated a null model under the assumption that spiking activity occurs randomly with respect to the DMR. We calculated this null model by first randomizing the inter-spike intervals and then averaging the spectrotemporal envelope of the DMR relative to the time of each spike. This generated a "noise" STRF. We repeated this procedure 1000× to generate a distribution of spectrotemporal noise-STRF samples. If a STRF sample was outside of the 99.9% confidence interval (i.e., $p<0.001$) of its respective noise-STRF sample, we considered it "significant"; if not, the STRF sample was assigned a value of 0.

For any given STRF, ~230 STRF samples (i.e., 288 temporal×800 spectral samples×0.001) were false positives. Although these samples exceeded our significance criterion, it did not fulfill our primary objective of identifying STRFs with reproducible and

JNeurosci Accepted Manuscript

reliable auditory responses. To identify such STRFs, we computed a “reliability” index by first breaking the DMR stimulus into twenty 30-s long segments (Escabi et al., 2014). Next, we randomly selected two subsamples of the 20 segments, generated a STRF from each of these segments, and calculated their Pearson correlation coefficient. A coefficient value of ~1 (0) indicated that a given STRF is reliable (not reliable). We repeated this procedure 500× to generate a distribution of correlation-coefficient values. Finally, we generated a null distribution of coefficient values using the same process but with randomized inter-spike intervals. A Mann-Whitney test evaluated the hypothesis that the actual and the null correlation-coefficient distributions had the same median values. If the null hypothesis was rejected ($p<0.01$), we considered a STRF to be statistically significant.

ANALYSIS OF SPIKING ACTIVITY ELICITED DURING THE PREDICTIVE-CODING PARADIGMS. To characterize the effect of the violations on neural activity, on a neuron-by-neuron basis, we computed a “response enhancement or suppression” (RESI) index: $RESI=(NR_2-NR_1)/(NR_2+NR_1)$, where NR_1 and NR_2 represent the mean firing rate elicited by the first and second tone burst, respectively, in a given tone-burst pair (see Fig. 2). We calculated the firing rate over a window extending from the onset of the tone burst to 50 ms after tone-burst offset. For the omission paradigm, we calculated the omitted response over an analogous time window. Next, we calculated the mean firing rate across all tone-burst pairs in a sequence. We generated two RESI values for the two tone-burst pattern sequences (expected and unexpected repetitions) and for the two tone-burst omission sequences (expected and unexpected omissions). Positive and negative RESI values imply repetition enhancement and suppression (e.g., stimulus-specific adaptation), respectively.

Finally, to quantify whether firing rate represented prediction errors in accordance with predictive coding theory, we computed a prediction-error index (PEI), which represents

JNeurosci Accepted Manuscript

the difference between the RESI value calculated for the violation condition (i.e., unexpected repetition and omission) and the standard condition (i.e., expected repetition and omission), respectively. PEI values ranged between -1 to +1. Values >0 indicate an enhanced response to the expectancy violation, consistent with predictive coding, whereas values ≤0 indicate a reduced response to the expectancy violation, inconsistent with predictive coding.

Statistical analyses

We used nonparametric tests on all analyses and null hypotheses were rejected at $p<0.05$.

JNeurosci Accepted Manuscript

Results

We report data from 198 single units that were recorded across 60 sessions from Monkey C and 229 single units that were recorded across 53 sessions from Monkey W. Because we did not record data from all 3 auditory paradigms (i.e., the oddball, pattern, and omission paradigms) during every recording session, the numbers of neurons across the different comparison groups are different. Nonetheless, in all sessions, we recorded data from at least 2 of the 3 auditory paradigms. Across different recording sessions, we modified the presentation rate of the tone bursts as well as the temporal occurrence of the tone burst that violated the expectation (e.g., in some sessions, it was presented randomly within a tone-burst sequence or at regular intervals). However, because our analyses indicated that these manipulations did not systematically change our neural population's responses to the tone burst that violated expectations, we combined the data in the presentation below; see the section entitled *Mixed evidence for and against PC theory in A1* below for further details. Also, because we did not identify a clear relationship between cortical depth and A1 responsivity to our stimulus paradigms, we pooled our recordings across cortical depth.

Current-source density (CSD) profiles and oddball responses are characteristic of the primary auditory cortex

We identified the primary auditory cortex (A1) through a series of functional assays, including the CSD profile (Steinschneider et al., 1992; Fishman et al., 2001b; Lakatos et al., 2005; Szymanski et al., 2009; Fishman and Steinschneider, 2010). The one-dimensional CSD profile was generated from the local-field potentials evoked by repetitively presented auditory stimuli and represents the laminar distribution of net transmembrane extracellular current flow associated with the synaptic activity of neural ensembles (Freeman and

JNeurosci Accepted Manuscript

Nicholson, 1975; Nicholson and Freeman, 1975; Muller-Preuss and Mitzdorf, 1984; Mitzdorf, 1985; Steinschneider et al., 1992).

Our CSD profiles displayed laminar patterns of net current sources and sinks co-located with multi-unit activity that were typical of A1 in awake macaques (Steinschneider et al., 1992; Fishman et al., 2001a; Lakatos et al., 2005; Fishman and Steinschneider, 2010; Banno et al., 2023; Cai et al., 2025). An example CSD profile is shown in Fig. 1C. This profile had a dipole pattern indicating net current influx that is characteristic of A1. In the middle electrode contacts, the CSD showed a sharp negative deflection (current sink; highlighted by arrow to the right of the CSD plot) soon after stimulus onset. In the same contacts, we also observed large increases in MUA (Fig. 1B). This large initial current sink, which typically coincided with the largest increases in MUA, is a characteristic feature of stimulus-evoked laminar response profiles in A1 and is consistent with post-synaptic depolarization of neural populations within putative input (granular) layers of the core auditory cortex (lamina 4 and lower lamina 3) (Steinschneider et al., 1992; Fishman et al., 2001b; Lakatos et al., 2005).

Furthermore, STRFs showed features that are typical of A1. Example STRFs from electrode contacts along a single penetration are shown in Fig. 1E. Similar to our previous reports and others (Miller et al., 2002; Fritz et al., 2003; Atencio and Schreiner, 2010; Cai et al., 2025), STRFs had short latencies with small circumscribed excitatory and/or inhibitory response fields. Moreover, we found that the best frequency (BF) of these STRFs was relatively constant along the electrode penetration (Cai et al., 2025). Our subsequent analyses include spiking activity obtained from all electrode contacts along the entire laminar extent of A1.

JNeurosci Accepted Manuscript

Mixed evidence for and against PC theory in A1

Consistent with previous studies that used the oddball paradigm (Fig. 2) in A1 (Ulanovsky et al., 2003; Farley et al., 2010; Fishman and Steinschneider, 2012; Natan et al., 2015; Parras et al., 2017), we found that the context of presentation modulated the neuron's response to the BF tone burst. Specifically, the firing rate was substantially higher when the BF tone burst was presented as the oddball (i.e., deviant stimulus) than when it was presented as the standard stimulus. Single-neuron examples are shown in Figs. 3A and 4A. On average, we found that deviant stimuli elicited significantly higher A1 firing rates than standard stimuli (H_0: median index value=0; the index is the difference between the deviant and standard firing rates, divided by their sum; Wilcoxon signed-rank test; Monkey W: N=61 single units; median [interquartile range, IQR]: 0.1 [-0.03-0.25]; $p<0.002$; Monkey C: N=38 single units; median [IQR]: 0.12 [−0.01-0.17]; $p<0.001$).

However, this pattern of responsivity is consistent with either reduced local suppression (e.g., due to SSA) or a prediction-error response as hypothesized by PC theory. To explore this issue further and to test these competing hypotheses, we probed A1 neurons with the pattern and omission paradigms (Fig. 2). Figs. 3-5 show the spiking patterns of three representative neurons recorded during the oddball, pattern, and omission paradigms.

During the pattern paradigm, A1 neurons responded robustly and equally well to both expected versus unexpected tone-burst repetitions (Figs. 3B and 5A). That is, the unexpected tone-burst repetition (which is a violation of the expectation for alternation; see Fig. 2) did not substantially modulate the neuron's firing rate. This finding is inconsistent with PC theory, which would predict a markedly larger response to the unexpected tone-burst repetition and would indicate the detection of a prediction error. In contrast, panels Figs. 4B and 5B show example response patterns during the omission paradigm. For these neurons,

JNeurosci Accepted Manuscript

we found slight increases in firing rate in response to the unexpected tone-burst omission relative to the expected tone-burst omission, consistent with PC theory.

The response patterns of these single-neuron examples are representative of our population findings (Figs. 6 and 7). To quantify these observations, we calculated a prediction-error index (PEI; see **Materials and Methods**). PEI values ranged between -1 to +1. Values >0 indicate an enhanced response to the expectancy violation, consistent with PC, whereas values <0 indicate reduced response to the expectancy violation, inconsistent with PC.

For the pattern paradigm (Fig. 6), the median PEI value was less than zero (H_0: median index value=0; Wilcoxon signed-rank test; Monkey W: N=79; -0.05 [-0.12-0.02]; p<0.00001; Monkey C: N=89; -0.04 [-0.13-0.03]; p<0.0011), which is inconsistent with PC theory. The data in Figs. S1 and S2 indicate that negative (median) PEI values were also found when we analyzed the pattern-paradigm data as a function of whether the deviant stimulus was presented randomly or at a fixed time within a tone-burst sequence (H_0: median index value=0; Wilcoxon signed-rank test; RANDOM: Monkey W: N=12; -0.12 [-0.16-0.02]; p<0.002; Monkey C; N=57; -0.04 [-0.14-0.03]; p<0.004; FIXED TIME: Monkey W; N=76; -0.02 [-0.11-0.029], p<0.007; Monkey C; N=38; -0.03 [-0.14-0.035], p<0.0374).

In contrast, for the omission paradigm (Fig. 7), the median PEI value was greater than zero (H_0: median index value=0; Wilcoxon signed-rank test; Monkey W: N=92; 0.05 [-0.004-0.12]; p<0.0001; Monkey C: N=71; 0.1 [0.01-0.24]; p<0.0001). This positive PEI value is consistent with PC theory and was observed both for random and fixed-time presentations of the deviant stimulus (Figs. S3 and S4; H_0: median index value=0; Wilcoxon signed-rank test; RANDOM: Monkey W: N=31; 0.06 [-0.002-0.14]; p<0.008; Monkey C; N=47; 0.09

JNeurosci Accepted Manuscript

[0.0003–0.29]; p<0.00001; FIXED TIME: Monkey W; N=82; -0.05 [-0.02-0.12], p<0.0001; Monkey C; N=26; -0.13 [0.02-0.27], p<0.0003).

The data in Figs. S1-S4. also illustrate the neuron-by-neuron relationship between the RESI values calculated from data collected during the standard and deviant versions of the pattern and omission paradigms (Fig. 2). In the analyses above, we reported the difference between these RESI values as the PEI value (see **Materials and Methods**). Neuron-by-neuron RESI values collapsed across both the pattern and omission paradigms are plotted in Fig. S5.

Strengthening our observation that A1 neurons differentially encoded deviant stimuli during the predictive and omission paradigms, a neuron-by-neuron analysis indicated that, on average, PEI values during the omission paradigm were larger than those during the pattern violation paradigm. This finding is shown in Fig. 8, where PEI values obtained from the spiking activity of single neurons during the omission paradigm are plotted against the PEI values obtained during the pattern paradigm. As can be seen, the majority of points lie below the line of equality, indicating that, on average, omission PEI values were greater than pattern PEI values (H_0: median difference between the paired omission and pattern PEI values is zero; Monkey W: N=29; 0.06 [-0.053 – 0.15]; p<0.03; Monkey C: N=52 units that were recorded in both conditions; 0.13 [0.0001-0.29]; p<0.00002).

Overall, our results indicate that the firing rates of individual A1 neurons are not enhanced for unexpected pattern violations and hence do not represent prediction errors. These findings are inconsistent with predictions of PC theory, but consistent with earlier preliminary findings in macaque A1 showing a similar absence of evidence for PC in neural population responses to unexpected stimulus repetitions (Fishman, 2014). On the other

JNeurosci Accepted Manuscript

hand, the firing rates of individual A1 neurons are enhanced during unexpected stimulus omissions, thus providing evidential support for PC theory.

In a final analysis, we tested the predictions of PC theory regarding the distribution of prediction-error neurons across cortical lamina. In line with several prominent PC models, we hypothesized that unexpected pattern violations registering as prediction errors would elicit increased spiking activity primarily in middle 'feedforward' cortical layers (Shipp, 2007; Friston, 2009; Arnal and Giraud, 2012; Bastos et al., 2012; Auksztulewicz and Friston, 2016; Shipp, 2016; Heilbron and Chait, 2018), whereas unexpected omissions of expected stimuli, which may index learned predictions, would elicit increased spiking activity primarily in superficial and deep cortical layers which are thought to receive and convey "feedback" activity from higher-order cortical areas (Shipp, 2007; Friston, 2009; Arnal and Giraud, 2012; Bastos et al., 2012; Auksztulewicz and Friston, 2016; Shipp, 2016; Heilbron and Chait, 2018). The results of this analysis are shown in Fig. 9 in which we plot the distribution of PEI values at different recording depths. Across both monkeys, we could not identify a pattern consistent with the aforementioned predictions of PC theory (H_0: median PEI values from the top (superficial), middle, and bottom (deep) third of recording locations were not significantly different; Kruskal-Wallis test; Monkey W: χ^2=0.53; p=0.7691; Monkey C: χ^2=8.24; p=0.0162). Further inspection of reliable group effect from Monkey C indicates that the median top- (superficial) and bottom- (deep) third PEI values were -0.03 and -0.05, respectively, whereas the middle third was -0.00044 with only the median deep and middle were reliably different (post-hoc comparison, Tukey-Kramer, p=0.0114). Thus, although there was a reliable group effect, because these median PEI values were less than zero, they were not consistent with PC theory.

JNeurosci Accepted Manuscript

We found a similar inconsistent pattern across monkeys for omission trials (H_0: median PEI values from the top (superficial), middle, and bottom (deep) third of recording locations were not significantly different; Kruskal-Wallis test; Monkey W: χ^2=6.26; p=0.0436; Monkey C: χ^2=0.29; p=0.863). However, although we found a reliable group effect for Monkey W, post-hoc comparisons (Tukey-Kramer, p>0.05) did not reveal specific group pairs driving the effect (median top- (superficial), middle-, and bottom- (deep) third PEI values were 0.024, 0.079 and 0.02, respectively).

JNeurosci Accepted Manuscript

Discussion

We tested whether there is evidence for the predictive-coding (PC) hypothesis in the primary auditory cortex (A1) of awake non-human primates. To isolate evidence for PC while controlling for SSA, we employed two auditory paradigms featuring unexpected pattern violations and unexpected stimulus omissions (Fishman, 2014). On average, A1 neurons were not modulated by expected versus unexpected stimulus repetitions (pattern violations), which is inconsistent with the predictions of PC. Conversely, and in line with PC, we found that A1 firing rates were higher for unexpected stimulus omissions compared to expected ones. Together, our findings provide nuanced evidence both for and against PC theory in A1.

Our results corroborate a substantial body of literature that has failed to find robust evidence for PC theory within A1, echoing previous findings of weak or absent prediction-error encoding during auditory-pattern violations (Farley et al., 2010; Fishman and Steinschneider, 2010, 2012; Fishman, 2014; Polterovich et al., 2018). That is, SSA and other lower-level phenomena, such as forward suppression, appear to play a predominant role in modulating responses to temporally structured stimulus patterns. Of course, our null result does not preclude evidence for PC in non-primary areas of auditory cortex, as reported in previous human and non-human primate studies (Wacongne et al., 2011; Todorovic and de Lange, 2012; Uhrig et al., 2014; Dürschmid et al., 2016; Parras et al., 2017; Nourski et al., 2018; Hofmann-Shen et al., 2020). Nonetheless, insofar as primary sensory cortical areas are thought to be involved in the neural circuitry underlying PC, our findings provide important constraints on the neurobiological implementation of the theory.

Furthermore, our finding of enhanced A1 responses to unexpected stimulus omissions supports previous findings in other animal models and in humans (Hughes et al.,

JNeurosci Accepted Manuscript

2001; Wacongne et al., 2011; Auksztulewicz et al., 2023; Cho et al., 2023; Lao-Rodríguez et al., 2023; Lao-Rodríguez et al., 2025; Yaron et al., 2025). Whereas our current data cannot map the circuitry underlying omission responses, they are thought to reflect top-down signals from higher-order regions that modulate sensory processing via feedback connections (Felleman and Van Essen, 1991; Shipp, 2007; Bastos et al., 2012; Markov and Kennedy, 2013; Chennu et al., 2016; Keller and Mrsic-Flogel, 2018; Bastos et al., 2020; Obara et al., 2023; Lao-Rodríguez et al., 2025).

The interpretation of these enhanced omission responses is complicated by several considerations. First, these enhanced responses may not only reflect prediction errors but could also reflect signatures of the top-down predictions (expectations) themselves (SanMiguel et al., 2013b; Kok et al., 2014; Schröger et al., 2015; Chennu et al., 2016; de Lange et al., 2018; Heilbron and Chait, 2018; Demarchi et al., 2019). On the other hand, these putative prediction signals, although consistent with PC, do not uniquely support PC theory, as responses to stimulus omissions may be related to other processes (Halpern and Zatorre, 1999; Zatorre and Halpern, 2005; Chennu et al., 2016; Marion et al., 2021). Another possibility is that omission responses reflect involuntary attentional mechanisms that prioritize the unexpected absence of stimuli for enhanced processing (Salmi et al., 2009; Noyce et al., 2023; Baragona et al., 2025; Lao-Rodríguez et al., 2025). In the future, it will be critical to compare A1 response profiles obtained using the present paradigms with those elicited by other control stimuli (e.g., “many standards” or “cascade”) to further differentiate predictive coding from ‘lower-level’ mechanisms such as stimulus-specific adaptation, forward suppression, etc. (Carbajal and Malmierca, 2018; Lao-Rodríguez et al., 2023; Lao-Rodríguez et al., 2025) and to gain further insight into whether these signals reflect PC or other possible neural models of Bayesian perceptual inference (Aitchison and Lengyel,

JNeurosci Accepted Manuscript

2017; Spratling, 2017; Heilbron and Chait, 2018; Keller and Mrsic-Flogel, 2018; Sohn and Narain, 2021; Lange et al., 2023).

Our finding of evidence for and against PC theory is consistent with a broad and diverse body of literature that has examined neural correlates of PC in other sensory cortices (Farley et al., 2010; Fishman and Steinschneider, 2012; Kaliukhovich and Vogels, 2014; Kok et al., 2014; Dürschmid et al., 2016; Rubin et al., 2016; Symonds et al., 2017; O'Reilly, 2021; Solomon et al., 2021; Tang et al., 2023; Dercksen et al., 2024; Han and Helmchen, 2024; Huang et al., 2024; Teichert et al., 2025). This complex picture may reflect multiple factors such as differences between stimulus paradigms and parameters, species differences, invasive versus non-invasive recordings of neural activity, the limitations of inferring underlying neural processes from non-invasively recorded brain signals, single-unit versus multiunit or neural ensemble measures, and/or differences between the responsivity of neural recordings in different cortical layers (Javitt et al., 1992; Fishman and Steinschneider, 2012; Aitken et al., 2020; Lakatos et al., 2020). It may also reflect the presence or absence of rigorous controls for lower-level phenomena such as stimulus-specific adaptation, forward suppression, and offset responses (May and Tiitinen, 2010; Fishman, 2014; Carbajal and Malmierca, 2018; O'Reilly and Conway, 2021; Nelken and Moshitch, 2026) as well as awake versus anesthetized conditions (Nourski et al., 2018; O'Reilly and Conway, 2021; Lao-Rodríguez et al., 2023), the degree and type of behavioral engagement (Nourski et al., 2021), and/or attentional effects (Kok et al., 2012; Smout et al., 2019).

Several potential limitations of the present study warrant consideration and further investigation in future research. First, because we focused our analyses on responses to BF tone bursts, it is possible that stronger evidence for PC during the pattern violation paradigm may be reflected in non-BF responses. Second, we might have found stronger neural

JNeurosci Accepted Manuscript

545 correlates of PC if the monkeys were actively engaged in a task as opposed to passive
546 listening (Fritz et al., 2003; Niwa et al., 2012; Atiani et al., 2014; Downer et al., 2015; Bagur
547 et al., 2018; Smout et al., 2019; Tsunada et al., 2019; Chillale et al., 2023; Male and O'Shea,
548 2023). Indeed, while prediction-error detection is traditionally seen as automatic and pre-
549 attentive (Tiitinen et al., 1994; Jacobsen and Schröger, 2001; Garrido et al., 2009), attention
550 can modulate the presence and magnitude of expectation, prediction, and prediction-error
551 signals in sensory cortices (Kok et al., 2012; Chennu et al., 2013; Auksztulewicz and Friston,
552 2015; Smout et al., 2019; Male and O'Shea, 2023; Baragona et al., 2025; Westerberg and
553 Roelfsema, 2026). Third, more robust signatures of PC may not be evident in single-unit
554 spiking activity but may be revealed in population-level activity such as local-field potentials
555 or neural ensemble activity (Fishman, 2014; Auksztulewicz et al., 2023). Fourth, because
556 we could not sufficiently distinguish between neural subtypes in our study, we could not
557 determine whether there was a relationship between RESI/PEI values and different
558 subtypes (e.g., excitatory versus inhibitory) (Shipp, 2016; Keller and Mrsic-Flogel, 2018;
559 Ross and Hamm, 2020). Relatedly, despite a large literature postulating such a relationship
560 (Friston, 2005; Shipp, 2007; Friston, 2009; Arnal and Giraud, 2012; Bastos et al., 2012;
561 Barto et al., 2013; Auksztulewicz and Friston, 2016; Shipp, 2016; de Lange et al., 2018;
562 Heilbron and Chait, 2018), we could not identify a consistent relationship between PEI
563 values and cortical depth (Fig. 9). Future studies should focus on exploring these
564 relationships in greater detail utilizing similar stimulus paradigms and/or active paradigms.
565 Finally, it remains an open question to what extent our findings obtained in macaques relate
566 to neural substrates of predictive processing, statistical learning, and perceptual inference
567 in humans. Addressing this limitation will require developing comparable experimental

JNeurosci Accepted Manuscript

568 paradigms and comparing similar measures of neural activity (e.g., single-unit activity or
569 local-field potentials) in both humans and non-human primates.
570

JNeurosci Accepted Manuscript

References

Aitchison L, Lengyel M (2017) With or without you: predictive coding and Bayesian inference in the brain. Current opinion in neurobiology 46:219-227.

Aitken F, Menelaou G, Warrington O, Koolschijn RS, Corbin N, Callaghan MF, Kok P (2020) Prior expectations evoke stimulus-specific activity in the deep layers of the primary visual cortex. PLoS biology 18:e3001023.

Alain C, Woods DL, Ogawa KH (1994) Brain indices of automatic pattern processing. Neuroreport 6:140-144.

Arnal LH, Giraud AL (2012) Cortical oscillations and sensory predictions. Trends in cognitive sciences 16:390-398.

Atencio CA, Schreiner CE (2010) Columnar connectivity and laminar processing in cat primary auditory cortex. PloS one 3:e9521.

Atiani S, David SV, Elgueda D, Locastro M, Radtke-Schuller S, Shamma SA, Fritz JB (2014) Emergent selectivity for task-relevant stimuli in higher-order auditory cortex. Neuron 82:486-499.

Auksztulewicz R, Friston K (2015) Attentional Enhancement of Auditory Mismatch Responses: a DCM/MEG Study. Cerebral cortex (New York, NY : 1991) 25:4273-4283.

Auksztulewicz R, Friston K (2016) Repetition suppression and its contextual determinants in predictive coding. Cortex 80:125-140.

JNeurosci Accepted Manuscript

Auksztulewicz R, Rajendran VG, Peng F, Schnupp JWH, Harper NS (2023) Omission responses in local field potentials in rat auditory cortex. BMC Biol 21:130.

Bagur S, Averseng M, Elgueda D, David S, Fritz J, Yin P, Shamma S, Boubenec Y, Ostojic S (2018) Go/No-Go task engagement enhances population representation of target stimuli in primary auditory cortex. Nature communications 9:2529.

Banno T, Shirley H, Fishman YI, Cohen YE (2023) Changes in neural readout of response magnitude during auditory streaming do not correlate with behavioral choice in the auditory cortex. Cell reports 42:113493.

Baragona V, Schröger E, Widmann A (2025) Salient, Unexpected Omissions of Sounds Can Involuntarily Distract Attention. Journal of cognitive neuroscience:1-16.

Barto A, Mirolli M, Baldassarre G (2013) Novelty or Surprise? Frontiers in psychology 4.

Bastos AM, Lundqvist M, Waite AS, Kopell N, Miller EK (2020) Layer and rhythm specificity for predictive routing. Proceedings of the National Academy of Sciences of the United States of America 117:31459-31469.

Bastos AM, Usrey WM, Adams RA, Mangun GR, Fries P, Friston KJ (2012) Canonical microcircuits for predictive coding. Neuron 76:695-711.

Bendixen A, Schroger E, Winkler I (2009) I heard that coming: event-related potential evidence for stimulus-driven prediction in the auditory system. The Journal of neuroscience : the official journal of the Society for Neuroscience 29:8447-8451.

JNeurosci Accepted Manuscript

610 Cai H, Shirley H, Escabí MA, Cohen YE (2025) Distinct Cortical Populations Drive
611 Multisensory Modulation of Segregated Auditory Sources. The Journal of
612 neuroscience : the official journal of the Society for Neuroscience 45.

613 Carbajal GV, Malmierca MS (2018) The Neuronal Basis of Predictive Coding Along the
614 Auditory Pathway: From the Subcortical Roots to Cortical Deviance Detection.
615 Trends Hear 22:2331216518784822.

616 Chandrasekaran C, Ghazanfar AA (2009) Different neural frequency bands integrate faces
617 and voices differently in the superior temporal sulcus. Journal of neurophysiology
618 101:773-788.

619 Chennu S, Noreika V, Gueorguiev D, Shtyrov Y, Bekinschtein TA, Henson R (2016) Silent
620 Expectations: Dynamic Causal Modeling of Cortical Prediction and Attention to
621 Sounds That Weren't. The Journal of neuroscience : the official journal of the Society
622 for Neuroscience 36:8305-8316.

623 Chennu S, Noreika V, Gueorguiev D, Blenkmann A, Kochen S, Ibáñez A, Owen AM,
624 Bekinschtein TA (2013) Expectation and attention in hierarchical auditory prediction.
625 The Journal of neuroscience : the official journal of the Society for Neuroscience
626 33:11194-11205.

627 Chiang CH, Lee J, Wang C, Williams AJ, Lucas TH, Cohen YE, Viventi J (2020) A modular
628 high-density µECoG system on macaque vlPFC for auditory cognitive decoding.
629 Journal of neural engineering 17:046008.

JNeurosci Accepted Manuscript

630 Chillale RK, Shamma S, Ostojic S, Boubenec Y (2023) Dynamics and maintenance of
631 categorical responses in primary auditory cortex during task engagement. eLife 12.

632 Cho H, Fonken YM, Adamek M, Jimenez R, Lin JJ, Schalk G, Knight RT, Brunner P (2023)
633 Unexpected sound omissions are signaled in human posterior superior temporal
634 gyrus: an intracranial study. Cerebral cortex (New York, NY : 1991) 33:8837-8848.

635 Christison-Lagay KL, Bennur S, Cohen YE (2017) Contribution of spiking activity in the
636 primary auditory cortex to detection in noise. J Neurophysiolology 118:3118-3131.

637 Cohen YE, Cohen IS, Gifford III GW (2004) Modulation of LIP activity by predictive auditory
638 and visual cues. Cerebral Cortex 14:1287-1301.

639 de Lange FP, Heilbron M, Kok P (2018) How Do Expectations Shape Perception? Trends
640 in cognitive sciences 22:764-779.

641 Demarchi G, Sanchez G, Weisz N (2019) Automatic and feature-specific prediction-related
642 neural activity in the human auditory system. Nature communications 10:3440.

643 Denham SL, Winkler I (2006) The role of predictive models in the formation of auditory
644 streams. Journal of physiology, Paris 100:154-170.

645 Dercksen TT, Widmann A, Noesselt T, Wetzel N (2024) Somatosensory omissions reveal
646 action-related predictive processing. Hum Brain Mapp 45:e26550.

647 Downer JD, Niwa M, Sutter ML (2015) Task engagement selectively modulates neural
648 correlations in primary auditory cortex. Journal Neuroscience 35:7565-7574.

JNeurosci Accepted Manuscript

649 Dürschmid S, Edwards E, Reichert C, Dewar C, Hinrichs H, Heinze HJ, Kirsch HE, Dalal
650 SS, Deouell LY, Knight RT (2016) Hierarchy of prediction errors for auditory events
651 in human temporal and frontal cortex. Proceedings of the National Academy of
652 Sciences of the United States of America 113:6755-6760.

653 Escabi MA, Read HL, Viventi J, Kim DH, Higgins NC, Storace DA, Liu AS, Gifford AM, Burke
654 JF, Campisi M, Kim YS, Avrin AE, Spiegel Jan V, Huang Y, Li M, Wu J, Rogers JA,
655 Litt B, Cohen YE (2014) A high-density, high-channel count, multiplexed muECoG
656 array for auditory-cortex recordings. Journal of neurophysiology 112:1566-1583.

657 Escabí MA, Schreiner CE (2002) Nonlinear spectrotemporal sound analysis by neurons in
658 the auditory midbrain. The Journal of neuroscience : the official journal of the Society
659 for Neuroscience 22:4114-4131.

660 Farley BJ, Quirk MC, Doherty JJ, Christian EP (2010) Stimulus-specific adaptation in
661 auditory cortex is an NMDA-independent process distinct from the sensory novelty
662 encoded by the mismatch negativity. The Journal of neuroscience : the official journal
663 of the Society for Neuroscience 30:16475-16484.

664 Felleman DJ, Van Essen DC (1991) Distributed hierarchical processing in the primate
665 cerebral cortex. Cerebral cortex (New York, NY : 1991) 1:1-47.

666 Fishman YI (2014) The mechanisms and meaning of the mismatch negativity. Brain
667 topography 27:500-526.

668 Fishman YI, Steinschneider M (2009) Temporally dynamic frequency tuning of population
669 responses in monkey primary auditory cortex. Hearing research 254:64-76.

JNeurosci Accepted Manuscript

Fishman YI, Steinschneider M (2010) Neural Correlates of Auditory Scene Analysis Based on Inharmonicity in Monkey Primary Auditory Cortex. Journal of Neuroscience 30:12480-12494.

Fishman YI, Steinschneider M (2012) Searching for the mismatch negativity in primary auditory cortex of the awake monkey: deviance detection or stimulus specific adaptation? The Journal of neuroscience : the official journal of the Society for Neuroscience 32:15747-15758.

Fishman YI, Reser DH, Arezzo JC, Steinschneider M (2001a) Neural correlates of auditory stream segregation in primary auditory cortex of the awake monkey. Hearing research 151:167-187.

Fishman YI, Volkov IO, Noh MD, Garell PC, Bakken H, Arezzo JC, Howard MA, Steinschneider M (2001b) Consonance and dissonance of musical chords: neural correlates in auditory cortex of monkeys and humans. J Neurophysiology 86:2761-2788.

Freeman JA, Nicholson C (1975) Experimental optimization of current source-density technique for anuran cerebellum. Journal of neurophysiology 38:369-382.

Frey S, Comeau R, Hynes B, Mackey S, Petrides M (2004) Frameless stereotaxy in the nonhuman primate. NeuroImage 23:1226-1234.

Friston K (2005) A theory of cortical responses. Philosophical transactions of the Royal Society of London Series B, Biological sciences 360:815-836.

JNeurosci Accepted Manuscript

690 Friston K (2009) The free-energy principle: a rough guide to the brain? Trends in cognitive
691 sciences 13:293-301.

692 Fritz J, Shamma S, Elhilali M, Klein D (2003) Rapid task-related plasticity of spectrotemporal
693 receptive fields in primary auditory cortex. Nature neuroscience 6:1216-1223.

694 Garrido MI, Kilner JM, Stephan KE, Friston KJ (2009) The mismatch negativity: a review of
695 underlying mechanisms. Clinical neurophysiology : official journal of the International
696 Federation of Clinical Neurophysiology 120:453-463.

697 Ghazanfar AA, Chandrasekaran C, Logothetis NK (2008) Interactions between the superior
698 temporal sulcus and auditory cortex mediate dynamic face/voice integration in
699 rhesus monkeys. The Journal of neuroscience : the official journal of the Society for
700 Neuroscience 28:4457-4469.

701 Ghazanfar AA, Maier JX, Hoffman KL, Logothetis NK (2005) Multisensory integration of
702 dynamic faces and voices in rhesus monkey auditory cortex. The Journal of
703 neuroscience : the official journal of the Society for Neuroscience 25:5004-5012.

704 Gifford AM, Sperling MR, Sharan A, Gorniak RJ, Williams RB, Davis K, Kahana MJ, Cohen
705 YE (2019) Neuronal phase consistency tracks dynamic changes in acoustic spectral
706 regularity. European Journal of Neuroscience 49:1268-1287.

707 Gold JI, Shadlen MN (2002) Banburismus and the brain: decoding the relationship beteween
708 sensory stimuli, decisions, and reward. Neuron 36:299-308.

709 Gold JI, Shadlen MN (2007) The Neural Basis of Decision Making. Annual review of
710 neuroscience 30:535-574.

JNeurosci Accepted Manuscript

711 Griffiths TL, Tenenbaum JB (2011) Predicting the future as Bayesian inference: people
712 combine prior knowledge with observations when estimating duration and extent. J
713 Exp Psychol Gen 140:725-743.

714 Halpern AR, Zatorre RJ (1999) When That Tune Runs Through Your Head: A PET
715 Investigation of Auditory Imagery for Familiar Melodies. Cerebral cortex (New York,
716 NY : 1991) 9:697-704.

717 Han S, Helmchen F (2024) Behavior-relevant top-down cross-modal predictions in mouse
718 neocortex. Nature neuroscience 27:298-308.

719 Heilbron M, Chait M (2018) Great Expectations: Is there Evidence for Predictive Coding in
720 Auditory Cortex? Neuroscience 389:54-73.

721 Hermes DJ, Aertsen AM, Johannesma PI, Eggermont JJ (1981) Spectrotemporal
722 characteristics of single units in the auditory midbrain of the lightly anesthetised
723 grass frog (*Rana temporaria* L.) investigated with tonal stimuli. Hearing research
724 6:103-126.

725 Hofmann-Shen C, Vogel BO, Kaffes M, Rudolph A, Brown EC, Tas C, Brüne M, Neuhaus
726 AH (2020) Mapping adaptation, deviance detection, and prediction error in auditory
727 processing. Neuroimage 207:116432.

728 Huang YT, Wu CT, Fang YM, Fu CK, Koike S, Chao ZC (2024) Crossmodal hierarchical
729 predictive coding for audiovisual sequences in the human brain. Commun Biol 7:965.

JNeurosci Accepted Manuscript

730 Hughes HC, Darcey TM, Barkan HI, Williamson PD, Roberts DW, Aslin CH (2001)
731 Responses of Human Auditory Association Cortex to the Omission of an Expected
732 Acoustic Event. NeuroImage 13:1073-1089.

733 Jacobsen T, Schröger E (2001) Is there pre-attentive memory-based comparison of pitch?
734 Psychophysiology 38:723-727.

735 Javitt DC, Schroeder CE, Steinschneider M, Arezzo JC, Vaughan HG, Jr. (1992)
736 Demonstration of mismatch negativity in the monkey. Electroencephalography and
737 clinical neurophysiology 83:87-90.

738 Johnston JM, Cohen YE, Shirley H, Tsunada J, Bennur S, Christison-Lagay K, Veeder CL
739 (2016) Recent refinements to cranial implants for rhesus macaques (Macaca
740 mulatta). Lab animal 45:180-186.

741 Kaliukhovich DA, Vogels R (2014) Neurons in macaque inferior temporal cortex show no
742 surprise response to deviants in visual oddball sequences. The Journal of
743 neuroscience : the official journal of the Society for Neuroscience 34:12801-12815.

744 Kayser C, Petkov CI, Logothetis NK (2007) Tuning to sound frequency in auditory field
745 potentials. Journal of neurophysiology 98:1806-1809.

746 Keller GB, Mrsic-Flogel TD (2018) Predictive Processing: A Canonical Cortical Computation.
747 Neuron 100:424-435.

748 Kim PJ, Young ED (1994) Comparative analysis of spectro-temporal receptive fields,
749 reverse correlation functions, and frequency tuning curves of auditory-nerve fibers.
750 The Journal of the Acoustical Society of America 95:410-422.

JNeurosci Accepted Manuscript

751 Knill DC, Richards W, eds (1996) Perception as (Bayesian) Inference. Cambridge, UK:
752 Cambridge University Press.

753 Koelsch S, Vuust P, Friston K (2019) Predictive Processes and the Peculiar Case of Music.
754 Trends in cognitive sciences 23:63-77.

755 Kok P, Failing MF, de Lange FP (2014) Prior expectations evoke stimulus templates in the
756 primary visual cortex. Journal of cognitive neuroscience 26:1546-1554.

757 Kok P, Rahnev D, Jehee JF, Lau HC, de Lange FP (2012) Attention reverses the effect of
758 prediction in silencing sensory signals. Cerebral cortex (New York, NY : 1991)
759 22:2197-2206.

760 Lakatos P, Shah AS, Knuth KH, Ulbert I, Karmos G, Schroeder CE (2005) An oscillatory
761 hierarchy controlling neuronal excitability and stimulus processing in the auditory
762 cortex. Journal of neurophysiology 94:1904-1911.

763 Lakatos P, O'Connell MN, Barczak A, McGinnis T, Neymotin S, Schroeder CE, Smiley JF,
764 Javitt DC (2020) The Thalamocortical Circuit of Auditory Mismatch Negativity. Biol
765 Psychiatry 87:770-780.

766 Lange RD, Shivkumar S, Chattoraj A, Haefner RM (2023) Bayesian encoding and decoding
767 as distinct perspectives on neural coding. Nature neuroscience 26:2063-2072.

768 Lao-Rodríguez AB, Schröger E, Malmierca MS (2025) The sound of silence: Omission
769 responses and how the brain predicts in the absence of sound. Neuroscience and
770 biobehavioral reviews 181:106505.

JNeurosci Accepted Manuscript

771 Lao-Rodríguez AB, Przewrocki K, Pérez-González D, Alishbayli A, Yilmaz E, Malmierca MS,
772 Englitz B (2023) Neuronal responses to omitted tones in the auditory brain: A
773 neuronal correlate for predictive coding. Sci Adv 9:eabq8657.

774 Liu X, Wan H, Shi L (2014) Quality metrics of spike sorting using neighborhood components
775 analysis. The open biomedical engineering journal 8:60-67.

776 Macdonald M, Campbell K (2011) Effects of a violation of an expected increase or decrease
777 in intensity on detection of change within an auditory pattern. Brain Cogn 77:438-
778 445.

779 Male AG, O'Shea RP (2023) Attention is required for canonical brain signature of prediction
780 error despite early encoding of the stimuli. PLoS biology 21:e3001866.

781 Marion G, Di Liberto GM, Shamma SA (2021) The Music of Silence: Part I: Responses to
782 Musical Imagery Encode Melodic Expectations and Acoustics. The Journal of
783 neuroscience : the official journal of the Society for Neuroscience 41:7435-7448.

784 Markov NT, Kennedy H (2013) The importance of being hierarchical. Current opinion in
785 neurobiology 23:187-194.

786 May PJ, Tiitinen H (2010) Mismatch negativity (MMN), the deviance-elicited auditory
787 deflection, explained. Psychophysiology 47:66-122.

788 May PJC (2021) The Adaptation Model Offers a Challenge for the Predictive Coding Account
789 of Mismatch Negativity. Frontiers in human neuroscience 15.

JNeurosci Accepted Manuscript

790 Miller LM, Escabí MA, Read HL, Schreiner CE (2001) Feature selectivity and interneuronal
791 cooperation in the thalamocortical system. The Journal of neuroscience : the official
792 journal of the Society for Neuroscience 21:8136-8144.

793 Miller LM, Escabí MA, Read HL, Schreiner CE (2002) Spectrotemporal receptive fields in
794 the lemniscal auditory thalamus and cortex. Journal of neurophysiology 87:516-527.

795 Mitzdorf U (1985) Current source-density method and application in cat cerebral cortex:
796 investigation of evoked potentials and EEG phenomena. Physiological reviews
797 65:37-100.

798 Muller-Preuss P, Mitzdorf U (1984) Functional anatomy of the inferior colliculus and the
799 auditory cortex: current source density analyses of click-evoked potentials. Hearing
800 research 16:133-142.

801 Natan RG, Briguglio JJ, Mwilambwe-Tshilobo L, Jones SI, Aizenberg M, Goldberg EM,
802 Geffen MN (2015) Complementary control of sensory adaptation by two types of
803 cortical interneurons. eLife 4.

804 Nelken I, Moshitch D (2026) How (not) to study deviance sensitivity and predictive coding in
805 auditory cortex. Hearing research 477:109672.

806 Nicholson C, Freeman JA (1975) Theory of current source-density analysis and
807 determination of conductivity tensor for anuran cerebellum. Journal of
808 neurophysiology 38:356-368.

JNeurosci Accepted Manuscript

809 Niwa M, Johnson JS, O'Connor KN, Sutter ML (2012) Active Engagement Improves Primary
810 Auditory Cortical Neurons' Ability to Discriminate Temporal Modulation. Journal of
811 Neuroscience 32:9323-9334.

812 Nourski KV, Steinschneider M, Rhone AE, Kawasaki H, Howard MA, 3rd, Banks MI (2018)
813 Auditory Predictive Coding across Awareness States under Anesthesia: An
814 Intracranial Electrophysiology Study. The Journal of neuroscience : the official
815 journal of the Society for Neuroscience 38:8441-8452.

816 Nourski KV, Steinschneider M, Rhone AE, Krause BM, Kawasaki H, Banks MI (2021)
817 Cortical responses to auditory novelty across task conditions: An intracranial
818 electrophysiology study. Hearing research 399:107911.

819 Noyce AL, Kwasa JAC, Shinn-Cunningham BG (2023) Defining attention from an auditory
820 perspective. Wiley Interdiscip Rev Cogn Sci 14:e1610.

821 O'Connell MN, Barczak A, Schroeder CE, Lakatos P (2014) Layer Specific Sharpening of
822 Frequency Tuning by Selective Attention in Primary Auditory Cortex. The Journal of
823 Neuroscience 34:16496-16508.

824 O'Reilly JA (2021) Roving oddball paradigm elicits sensory gating, frequency sensitivity, and
825 long-latency response in common marmosets. IBRO Neurosci Rep 11:128-136.

826 O'Reilly JA, Conway BA (2021) Classical and controlled auditory mismatch responses to
827 multiple physical deviances in anaesthetised and conscious mice. The European
828 journal of neuroscience 53:1839-1854.

JNeurosci Accepted Manuscript

Obara K, Ebina T, Terada SI, Uka T, Komatsu M, Takaji M, Watakabe A, Kobayashi K, Masamizu Y, Mizukami H, Yamamori T, Kasai K, Matsuzaki M (2023) Change detection in the primate auditory cortex through feedback of prediction error signals. Nature communications 14:6981.

Paavilainen P (2013) The mismatch-negativity (MMN) component of the auditory event-related potential to violations of abstract regularities: a review. International journal of psychophysiology : official journal of the International Organization of Psychophysiology 88:109-123.

Pachitariu M, Steinmetz N, Kadir S, Carandini M, Harris KD (2023) Kilosort: realtime spike-sorting for extracellular electrophysiology with hundreds of channels. bioRxiv:061481.

Parras GG, Nieto-Diego J, Carbajal GV, Valdés-Baizabal C, Escera C, Malmierca MS (2017) Neurons along the auditory pathway exhibit a hierarchical organization of prediction error. Nature communications 8:2148.

Polterovich A, Jankowski MM, Nelken I (2018) Deviance sensitivity in the auditory cortex of freely moving rats. PloS one 13:e0197678.

Rao RPN, Ballard DH (1999) Predictive coding in the visual cortex: a functional interpretation of some extra-classical receptive-field effects. Nature neuroscience 2:79-87.

Romanski LM, Goldman-Rakic PS (2002) An auditory domain in primate prefrontal cortex. Nature neuroscience 5:15-16.

JNeurosci Accepted Manuscript

Ross JM, Hamm JP (2020) Cortical Microcircuit Mechanisms of Mismatch Negativity and Its Underlying Subcomponents. Frontiers in neural circuits 14:13.

Rubin J, Ulanovsky N, Nelken I, Tishby N (2016) The Representation of Prediction Error in Auditory Cortex. PLoS computational biology 12:e1005058.

Salmi J, Rinne T, Koistinen S, Salonen O, Alho K (2009) Brain networks of bottom-up triggered and top-down controlled shifting of auditory attention. Brain research 1286:155-164.

Sanmiguel I, Saupe K, Schröger E (2013a) I know what is missing here: electrophysiological prediction error signals elicited by omissions of predicted "what" but not "when". Frontiers in human neuroscience 7:407.

SanMiguel I, Widmann A, Bendixen A, Trujillo-Barreto N, Schröger E (2013b) Hearing silences: human auditory processing relies on preactivation of sound-specific brain activity patterns. The Journal of neuroscience : the official journal of the Society for Neuroscience 33:8633-8639.

Schmitzer-Torbert N, Jackson J, Henze D, Harris K, Redish AD (2005) Quantitative measures of cluster quality for use in extracellular recordings. Neuroscience 131:1-11.

Schröger E, Marzecová A, SanMiguel I (2015) Attention and prediction in human audition: a lesson from cognitive psychophysiology. The European journal of neuroscience 41:641-664.

JNeurosci Accepted Manuscript

869 Shipp S (2007) Structure and function of the cerebral cortex. Current biology : CB 17:R443-
870 R339.

871 Shipp S (2016) Neural Elements for Predictive Coding. Frontiers in psychology 7:1792.

872 Smout CA, Tang MF, Garrido MI, Mattingley JB (2019) Attention promotes the neural
873 encoding of prediction errors. PLoS biology 17:e2006812.

874 Sohn H, Narain D (2021) Neural implementations of Bayesian inference. Current opinion in
875 neurobiology 70:121-129.

876 Solomon SS, Tang H, Sussman E, Kohn A (2021) Limited Evidence for Sensory Prediction
877 Error Responses in Visual Cortex of Macaques and Humans. Cerebral cortex (New
878 York, NY : 1991) 31:3136-3152.

879 Spratling MW (2017) A review of predictive coding algorithms. Brain Cogn 112:92-97.

880 Steinschneider M, Fishman YI, Arezzo J, C. (2008) Spectrotemporal analysis of evoked and
881 induced electroencephalographic responses in primary auditory cortex (A1) of the
882 awake monkey. Cerebral cortex (New York, NY : 1991) 18:610-625.

883 Steinschneider M, Tenke CE, Schroeder CE, Javitt DC, Simpson GV, Arezzo JC, Vaughan
884 HG, Jr. (1992) Cellular generators of the cortical auditory evoked potential initial
885 component. Electroencephalography and clinical neurophysiology 84:196-200.

886 Symonds RM, Lee WW, Kohn A, Schwartz O, Witkowski S, Sussman ES (2017)
887 Distinguishing Neural Adaptation and Predictive Coding Hypotheses in Auditory
888 Change Detection. Brain topography 30:136-148.

JNeurosci Accepted Manuscript

889 Szabó BT, Denham SL, Winkler I (2016) Computational Models of Auditory Scene Analysis:
890 A Review. Frontiers in Neuroscience Volume 10 - 2016.

891 Szymanski FD, Garcia-Lazaro JA, Schnupp JW (2009) Current source density profiles of
892 stimulus-specific adaptation in rat auditory cortex. Journal of neurophysiology
893 102:1483-1490.

894 Tang MF, Kheradpezhouh E, Lee CCY, Dickinson JE, Mattingley JB, Arabzadeh E (2023)
895 Expectation violations enhance neuronal encoding of sensory information in mouse
896 primary visual cortex. Nature communications 14:1196.

897 Teichert T, Jedema H, Zhen Z, Gurnsey K (2025) Complementary functional profiles of
898 mismatch responses mediated by adaptation and deviance detection point to two
899 distinct auditory short-term memory systems. Journal of neurophysiology 134:314-
900 336.

901 Tiitinen H, May P, Reinikainen K, Naatanen R (1994) Attentive novelty detection in humans
902 is governed by pre-attentive sensory memory. Nature 372:90-92.

903 Todorovic A, de Lange FP (2012) Repetition suppression and expectation suppression are
904 dissociable in time in early auditory evoked fields. The Journal of neuroscience : the
905 official journal of the Society for Neuroscience 32:13389-13395.

906 Tsunada J, Cohen Y, Gold JI (2019) Post-decision processing in primate prefrontal cortex
907 influences subsequent choices on an auditory decision-making task. eLife 8:e46770.

JNeurosci Accepted Manuscript

908 Tsunada J, Baker AE, Christison-Lagay KL, Davis SJ, Cohen YE (2011) Modulation of cross-
909 frequency coupling by novel and repeated stimuli in the primate ventrolateral
910 prefrontal cortex. Front Psychology 2.

911 Uhrig L, Dehaene S, Jarraya B (2014) A hierarchy of responses to auditory regularities in
912 the macaque brain. The Journal of neuroscience : the official journal of the Society
913 for Neuroscience 34:1127-1132.

914 Ulanovsky N, Las L, Nelken I (2003) Processing of low-probability sounds by cortical
915 neurons. Nature neuroscience 6:391-398.

916 Wacongne C, Changeux JP, Dehaene S (2012) A neuronal model of predictive coding
917 accounting for the mismatch negativity. The Journal of neuroscience : the official
918 journal of the Society for Neuroscience 32:3665-3678.

919 Wacongne C, Labyt E, van Wassenhove V, Bekinschtein T, Naccache L, Dehaene S (2011)
920 Evidence for a hierarchy of predictions and prediction errors in human cortex.
921 Proceedings of the National Academy of Sciences of the United States of America
922 108:20754-20759.

923 Westerberg JA, Roelfsema PR (2026) Hierarchical interactions between sensory cortices
924 defy predictive coding. Trends in cognitive sciences 30:110-123.

925 Yaron A, Shiramatsu-Isoguchi T, Kern FB, Ohki K, Takahashi H, Chao ZC (2025) Auditory
926 cortex neurons that encode negative prediction errors respond to omissions of
927 sounds in a predictable sequence. PLoS biology 23:e3003242.

INeurosci Accepted Manuscript

928 Zarcone A, van Schijndel M, Vogels J, Demberg V (2016) Salience and Attention in
929 Surprisal-Based Accounts of Language Processing. Frontiers in psychology Volume
930 7 - 2016.

931 Zatorre RJ, Halpern AR (2005) Mental concerts: musical imagery and auditory cortex.
932 Neuron 47:9-12.

933

934

JNeurosci Accepted Manuscript

Figure Legends

Figure 1: Representative laminar response profile and spectrotemporal response fields from A1. As a function of cortical depth from the superficial (top) to the deep (bottom) layers, we plot **(A)** the auditory evoked potentials (AEPs), which are derived from local-field potentials, **(B)** multiunit activity (MUA), and **(C)** the one-dimensional current source density (CSD), which is derived from the AEP profile. An arrow indicates the sharp negative deflection of a current sink in the middle channels. The laminar AEP, MUA, and CSD profiles are comprised of alternate electrode channels (200-μm rather than 100-μm inter-contact spacing) to enhance the visualization of major response components and facilitate comparison with profiles shown in previous studies (Fishman et al., 2001a; Fishman et al., 2001b; Lakatos et al., 2005; Fishman and Steinschneider, 2009, 2010, 2012; Fishman, 2014; O'Connell et al., 2014). **(D)** Significant single-unit STRFs obtained from different electrode contacts during the same recording session. Arrows indicate the locations of the electrode contacts that had significant STRFs. The x-axis is aligned relative to stimulus onset. Color indicates the probability of eliciting a spike at each time-frequency point (red: maximum probability of eliciting a spike; blue: minimum probability of eliciting a spike; see color bar).

Figure 2: Schematic representation of the three auditory paradigms. Tone bursts are represented as “notes” with standard tone bursts represented in black and unexpected tone bursts in red. For the pattern paradigm that tested for unexpected repetition, the tone burst in grey indicates that it has a different frequency than the standard

JNeurosci Accepted Manuscript

tone burst. For the omission paradigm, the asterisk represents the expected (black) or the unexpected (red) missing tone burst.

Figure 3: Raster and peristimulus-time histogram from a single neuron recorded during the oddball and pattern paradigms. **(A)** For the oddball paradigm, the raster plots and histograms are aligned relative to the onset of each tone burst. **(B)** For the pattern paradigm, the raster plots are aligned relative to the onset of each tone-burst pair. In both panels, the data in the left and right columns are data from the expected and unexpected conditions, respectively. The grey bars indicate the time course of a tone burst.

Figure 4: Raster and peristimulus-time histogram from a single neuron recorded during the oddball and omission paradigms. **(A)** For the oddball paradigm, the raster plots and histograms are aligned relative to the onset of each tone burst. **(B)** For the omission paradigm, the raster plots are aligned relative to the onset of the tone-burst + omitted-tone-burst complex. In both panels, the data in the left and right columns are data from the expected and unexpected conditions, respectively. The grey bars indicate the time course of a tone burst, whereas the black bars indicate the “time course” of the missing tone burst.

Figure 5: Raster and peristimulus-time histogram from a single neuron recorded during the pattern and omission paradigms. **(A)** For the pattern paradigm, the raster plots are aligned relative to the onset of each tone-burst pair. **(B)** For the omission paradigm, the raster plots are aligned relative to the onset of each tone-burst pair or tone-burst + omitted tone-burst complex. In both panels, the data in the left and right columns are

JNeurosci Accepted Manuscript

data from the expected and unexpected conditions, respectively. The grey bars indicate the time course of a tone burst, whereas the black bars indicate the “time course” of the missing tone burst.

Figure 6: Distribution of PEI values during the pattern paradigm. PEI values >0 are consistent with predictive coding. The solid vertical line in each histogram indicates PEI=0. The data in **(A)** are from monkey C, whereas the data in **(B)** are from monkey W.

Figure 7: Distribution of PEI values during the omission paradigm. PEI values >0 are consistent with predictive coding. The solid vertical line in each histogram indicates PEI=0. The data in **(A)** are from monkey C, whereas the data in **(B)** are from monkey W.

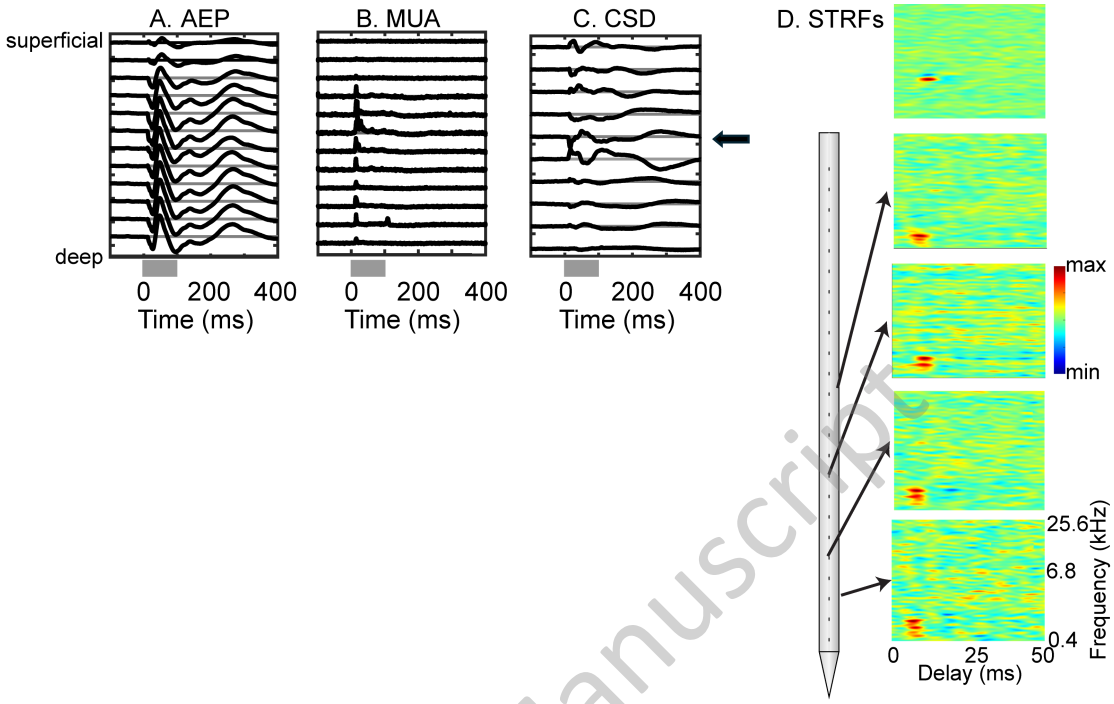
Figure 8: Correlation analysis of PEI values. On a neuron-by-neuron basis, the PEI values from the omission paradigm are plotted on the x-axis and the PEI values from the pattern paradigm are plotted on the y-axis. The data in **(A)** are from monkey C, whereas the data in **(B)** are from monkey W. The solid line in both panels is the line of unity. Note: the appearance of grey and black circles is an artifact of the overlapping data points rather than differences in tuning, responsivity, etc.

Figure 9: Distribution of PEI values across recording depth. On a session-by-session basis, PEI values are plotted as a function of recording depth from superficial (top) to deep (bottom) layers. Recording depth is aligned relative to the CSD current sink; see Fig. 1. Each horizontal violin represents the distribution of PEI values at each electrode channel (depth) with individual session PEI values overlaid as open circles. The vertical

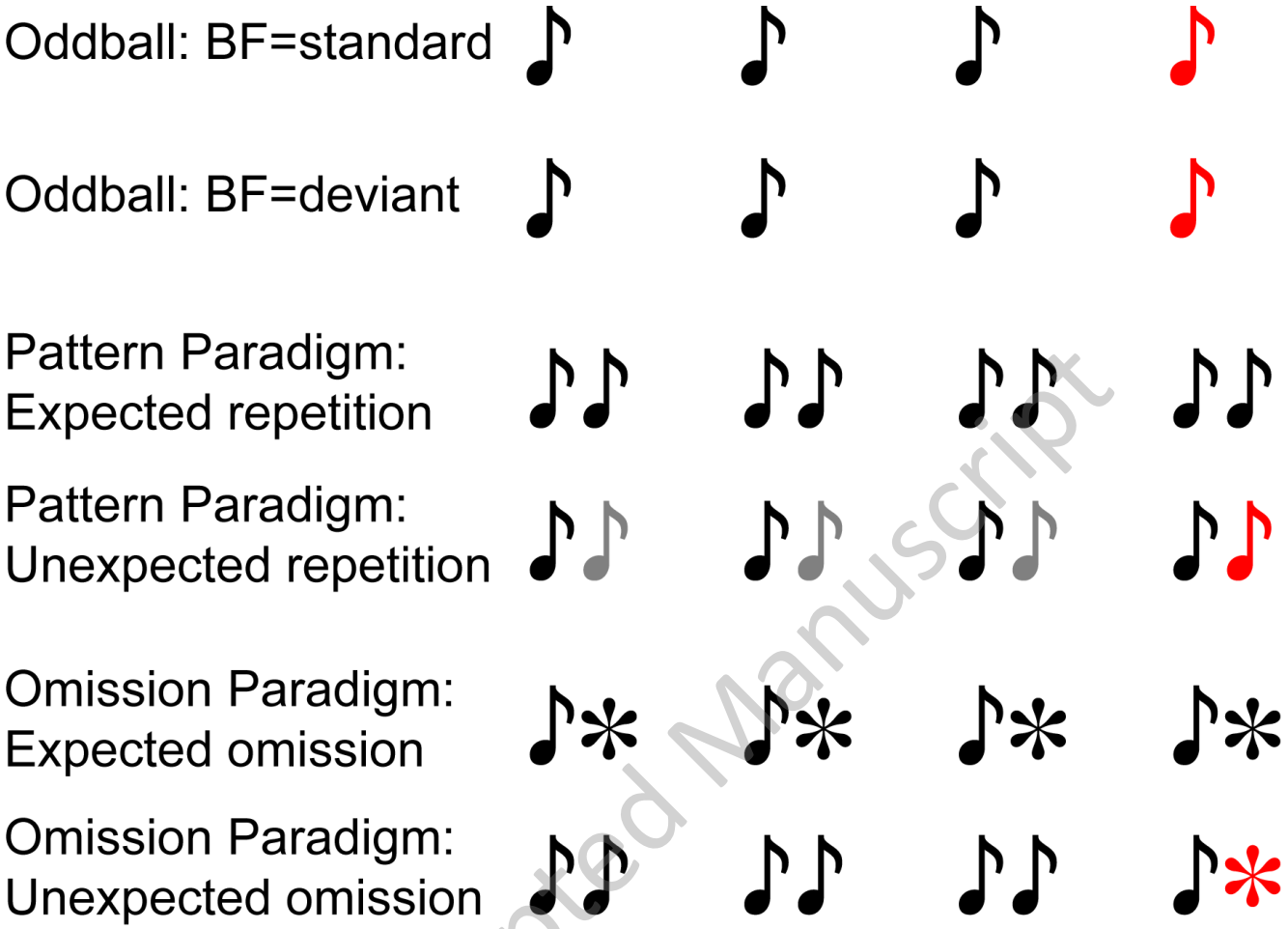
JNeurosci Accepted Manuscript

dashed line indicates a PEI value of 0. Data in the **top** and **bottom** panels relate to the pattern-violation paradigm and omission paradigm, respectively. Data in the **left** and **right** columns are from Monkey C and Monkey W, respectively.

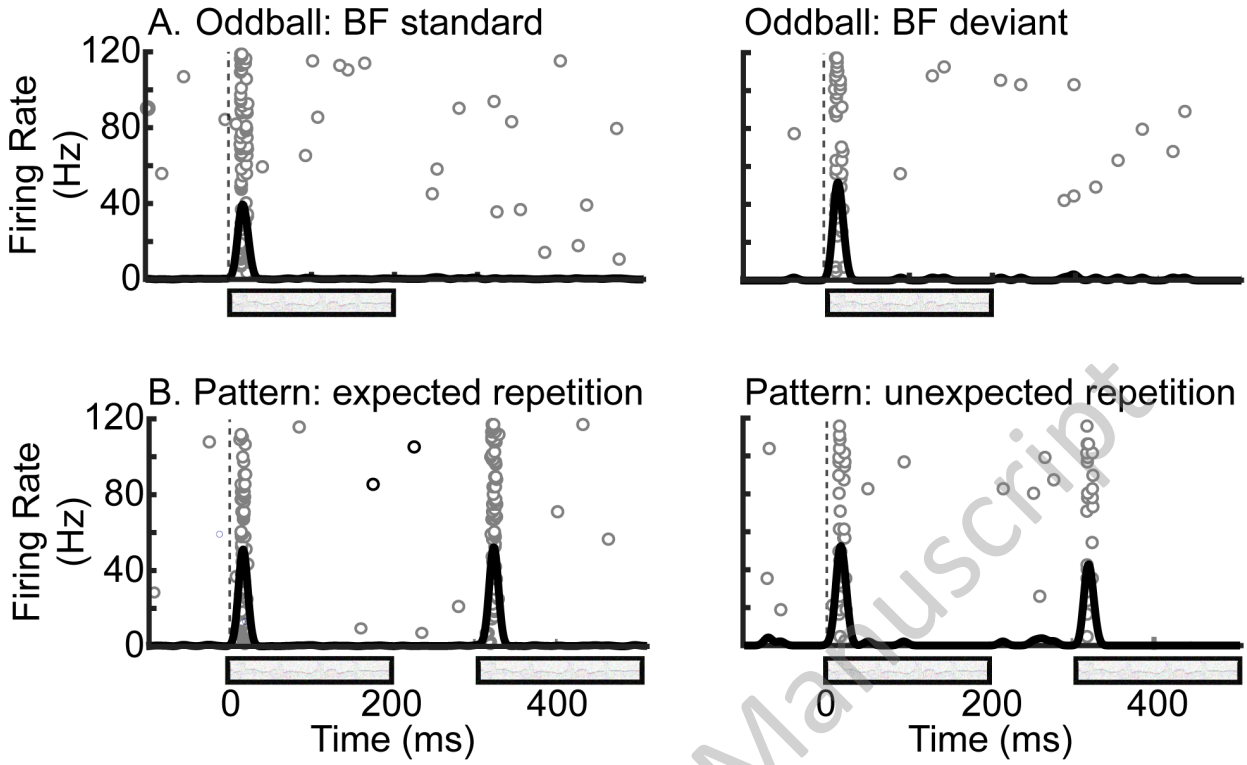
JNeurosci Accepted Manuscript



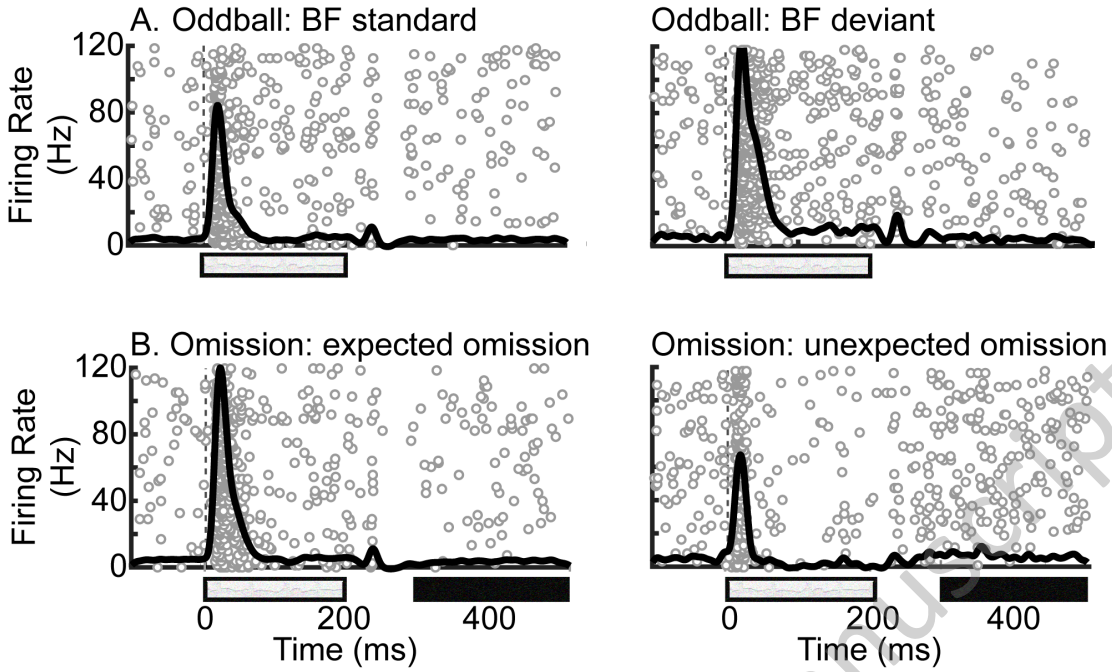
JNeurosci Accepted Manuscript



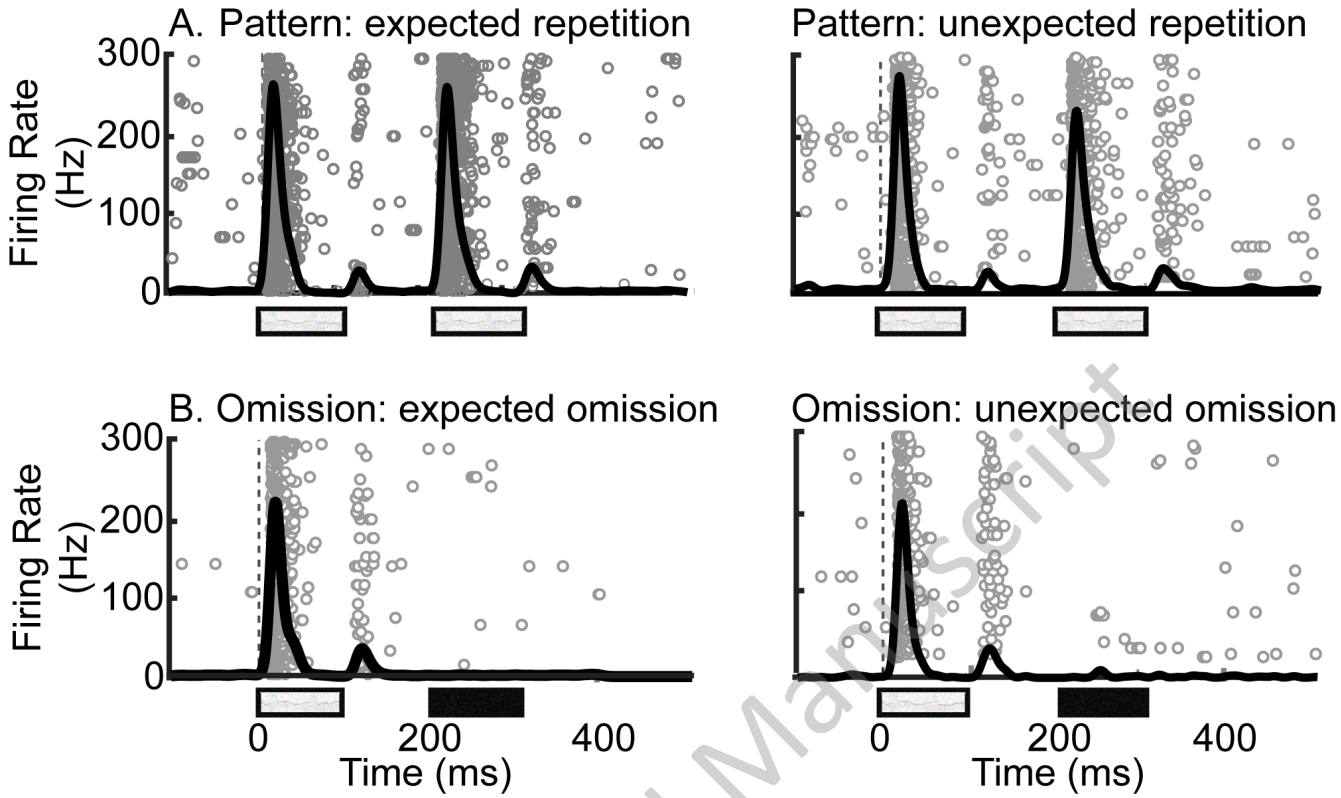
JNeurosci Accepted Manuscript



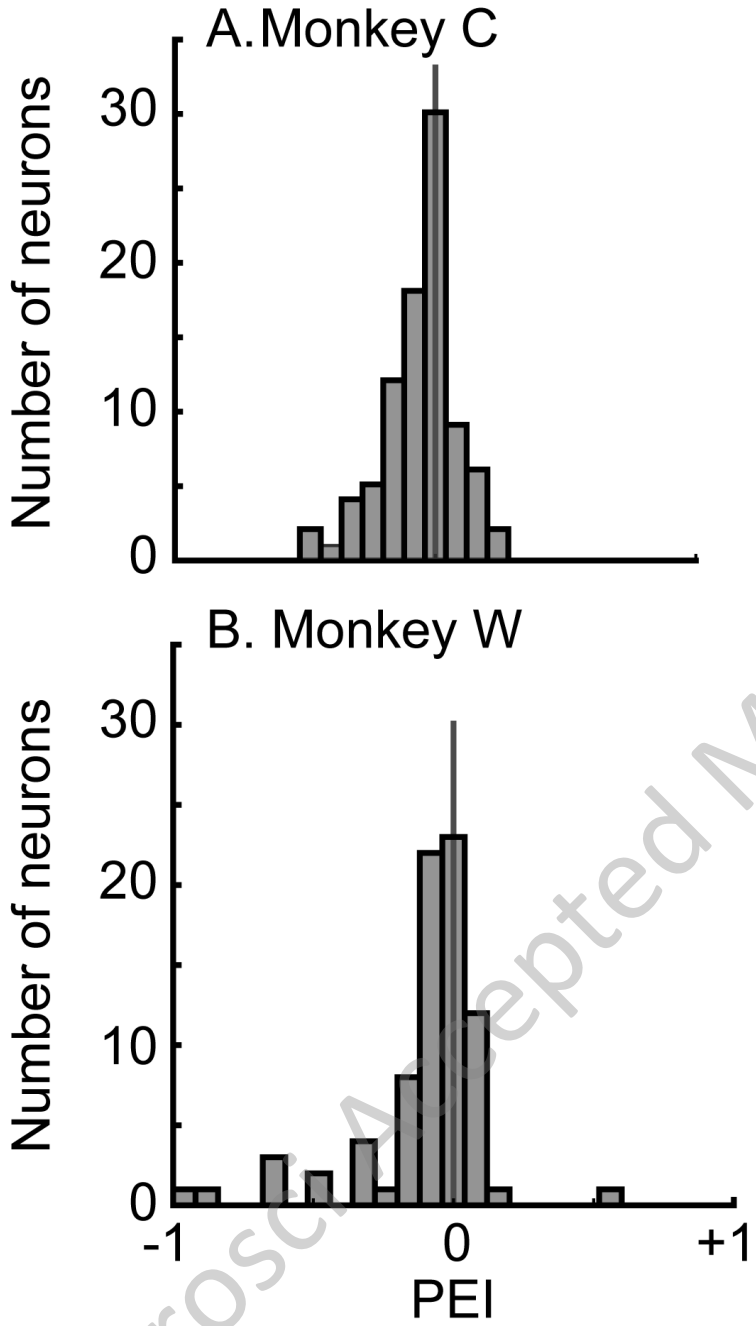
JNeurosci Accepted Manuscript



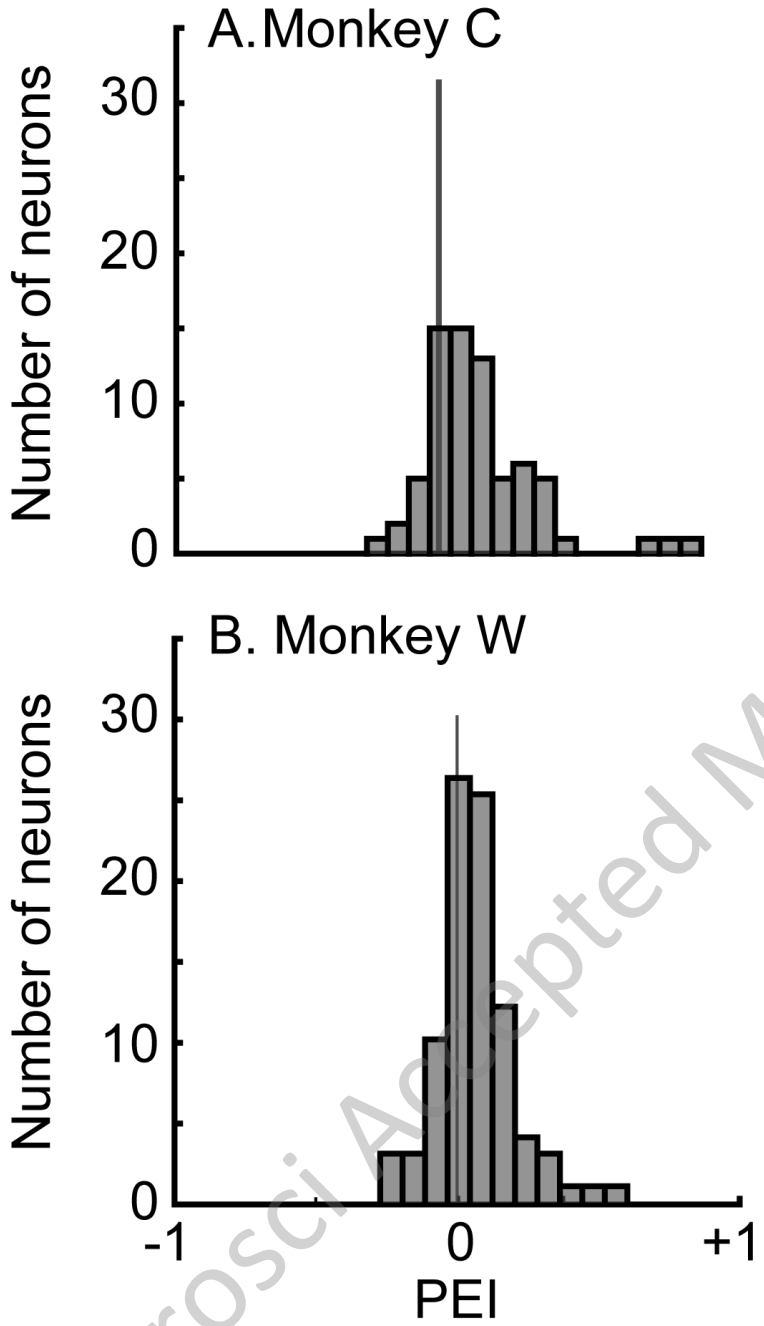
JNeurosci Accepted Manuscript



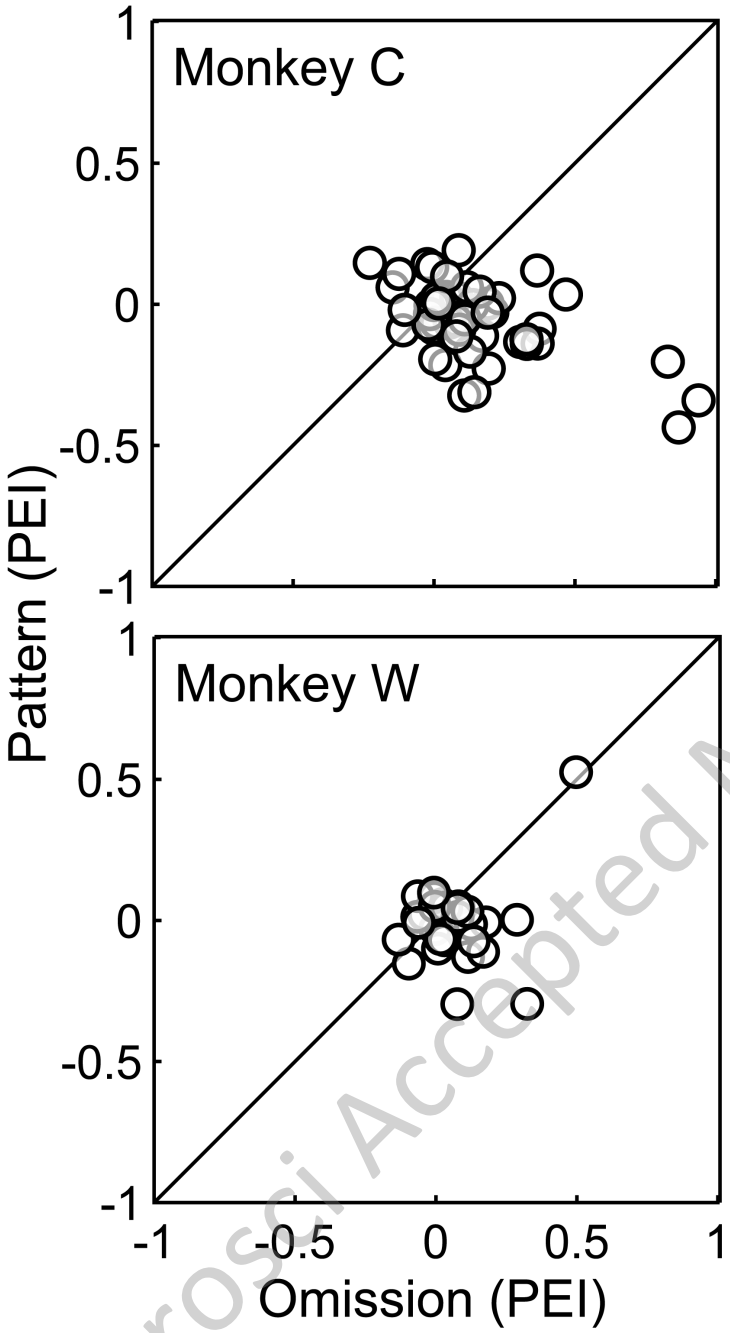
JNeurosci Accepted Manuscript



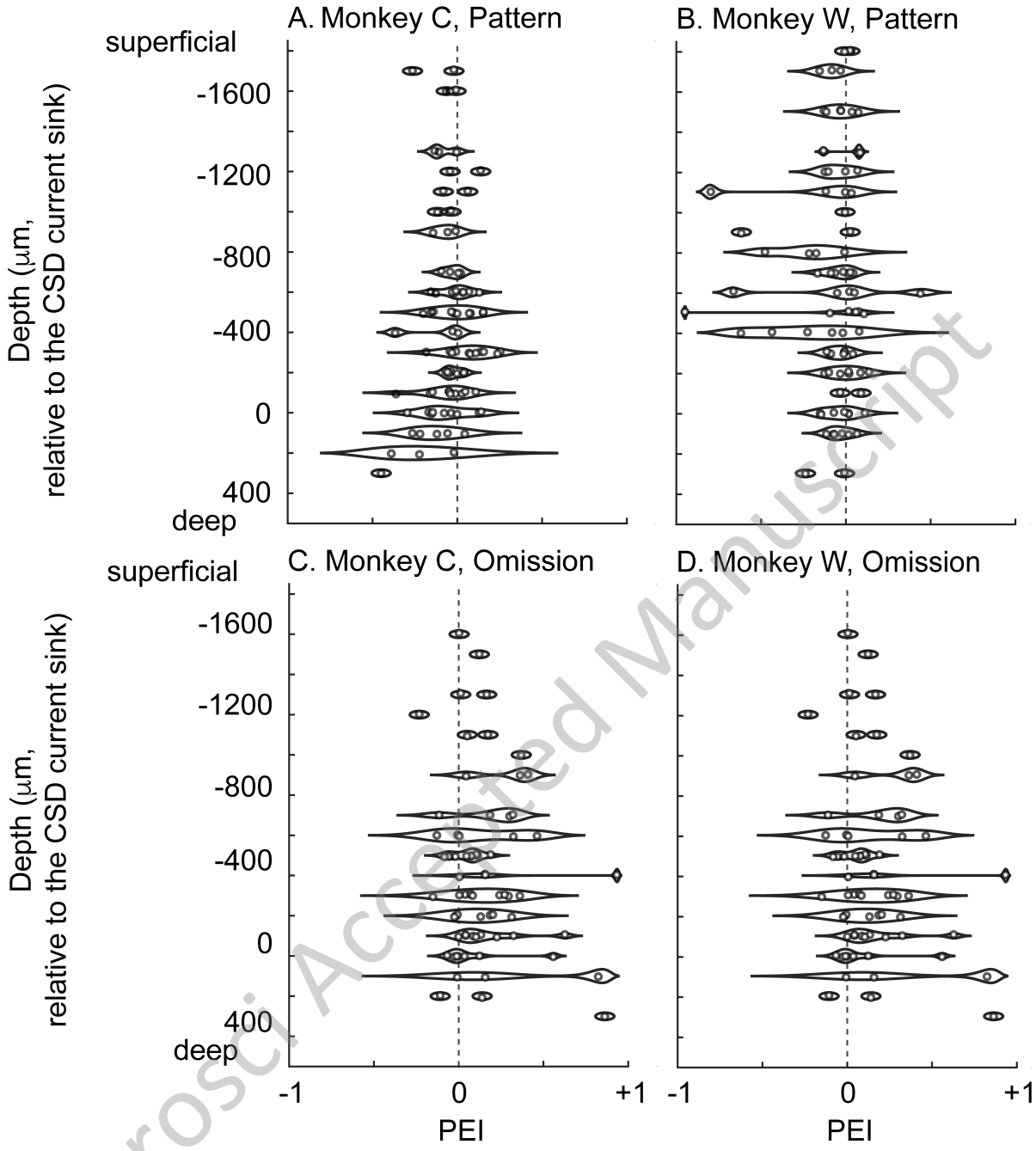
JNeurosci Accepted Manuscript



JNeurosci Accepted Manuscript



JNeurosci Accepted Manuscript



JNeurosci Accepted Manuscript